Angle Resolved Scattering Measurement of Multiple Spherical Particles by Fourier Transform

Jian Zhang, Chengzhuang Zhou, Xiaolong Li, and Datong Wu

***Abstract*—In this paper, we report that the far field diffraction pattern of a specimen which is consisting of an array of spherical particles enables the determination of the size and refractive index of each scattering sphere. The far field 2D angular resolved diffraction pattern, of which the diffraction angle reaches tens of degrees, is measured by CCD camera. On one hand, the diffraction pattern distorted obviously at high angles is corrected for curvature. The amplitude and phase images of the specimen are reconstructed by difference map iterative algorithm. The size of each scattering microsphere is calculated according to its pixel numbers and the image resolution. On the other hand, the diffraction pattern without curvature correction is used to reconstruct the amplitude and phase images of the specimen by HIO algorithm. The amplitude and phase images of each sphere are isolated. Then the angular resolved scattering signals of the individual spheres are quantitatively indicated by Fourier transform. Finally, the refractive index of each microsphere is obtained by fitting the experimental results using Mie theory.**

***Index Terms*—Scattering measurements, scattering particles.**

I. Introduction

THE scattering properties of single or multiple microspheres are important to broad applications in many fields of science, such as optical ultramicroscopy, atmospheric science and colloid physics [1]–[3]. These applications rely on the sizes and refractive indices of microspheres, which are the information contained in the scattering signals [4]. With the benefits of fast measurement and calculation, the digital holography method is widely used to determine the sizes and refractive indices of microspheres. However, this method needs to know the nature of the reference light, which is difficult to achieve in some cases. In addition, the digital holography cannot obtain the complicated scattering signal of a multiple micro particles system, which redistributes the optical field [5], [6]. Thus using digital holography to measure the microspheres faces the problem to optimize more than one parameter simultaneously, which yields inaccurate results. In this paper, we investigated microspheres with coherent diffraction imaging, which phases the image by oversampling method and iterative algorithm. The diffraction patterns at both low and high angles were directly recorded avoiding the interference between direct beam and diffraction signals.

Manuscript received May 1, 2021; revised June 20, 2021; accepted June 25, 2021. Date of publication June 29, 2021; date of current version July 16, 2021. *(Corresponding author: Jian Zhang.)*

The authors are with the School of Science, Shandong Jianzhu University, Jinan 250101, China (e-mail: jianzhang_sdjzu@163.com; 1429161398@qq.com; 17865311958@163.com; yy672706339@163.com).

Digital Object Identifier 10.1109/JPHOT.2021.3093477

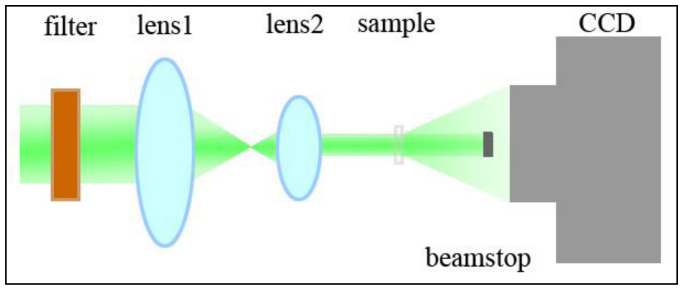

Fig. 1. Schematic layout of the experimental setup.

To our knowledge, it is a challenge to obtain the size and refractive index of each microsphere in a multiple particles system only using the diffraction pattern and the Mie theory. Here, taking advantages of quantifiability of coherent diffraction imaging, we demonstrated that the size and refractive index of each sphere can be determined by Fourier transform of the diffraction pattern of multiple spherical particles. Diffraction patterns were recorded by a charge-coupled-device (CCD) camera. The image of the specimen was reconstructed twice. The image was first reconstructed by the diffraction pattern after curvature correction. Then, the size of a microsphere was calculated according to the resolution of the diffraction pattern and the number of pixels of the microsphere without any priori information of the refractive index. The diffraction pattern without curvature correction was then used to reconstruct the image of the specimen. To isolate the amplitude and phase of the individual spheres, a convolution of the reconstructed image was performed and a cutoff value was set. The angular resolved scattering signal of each sphere was obtained by Fourier transform. Finally, the refractive indices of the microspheres were obtained by using the Mie theory to fit the experimental results with the sizes of the microspheres that had been calculated.

II. Experimental Details

The schematic layout of experimental arrangement is shown in Fig. 1. In this configuration, the light source was a He-Ne laser at a wavelength of 543 nm. The beam was first attenuated by an absorption neutral attenuator. Two converging lenses were used to focus the beam to a spot for improving the luminous flux. The focal lengths of the lens 1 and the lens 2 are 1500 millimeters and 500 millimeters. The specimen was a collection of porous silica microspheres, mounted on a glass coverslip, to form a running person. It was about 147 μm tall $\times$ 130 μm wide, as shown in

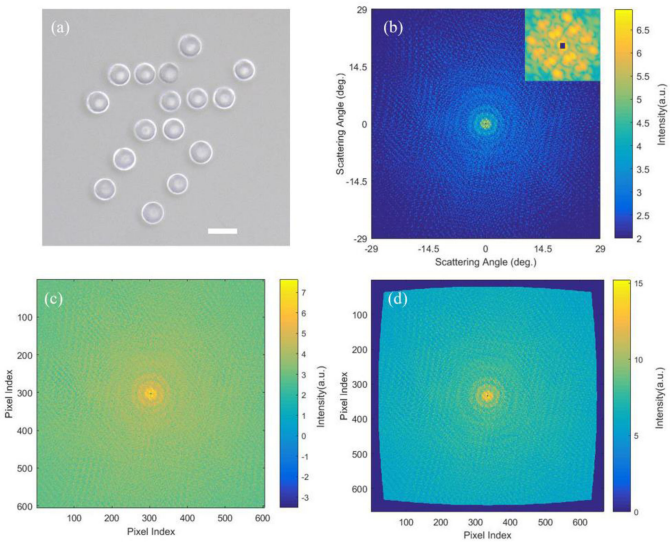

Fig. 2. (a) Specimen composed of several porous silica spheres deposited on a glass coverslip. (b) Diffraction pattern of the specimen before curvature correction. (c) Diffraction pattern after binning and deconvolution. (d) Diffraction pattern after curvature correction. Inset in part (b): Central speckle with missing data induced by a beam stop. The scale bar in (a) is 20 microns.

Fig. 2(a). The diameter of each microsphere was ∼20 microns which is given by the manufacturer. The specimen was placed at the waist of the beam to satisfy the approximation of planar wave. A beam with a small diameter ∼500 microns was incident on the specimen. An adjustable aperture was mounted downstream of the specimen for cleaning the stray light from other upstream optical devices. For avoiding saturation, a beam stop was placed upstream of the specimen. A liquid-nitrogen-cooled CCD with pixel size of 20 μm × 20 μm in a 1300 × 1340 array was used to record the diffraction patterns.

First, to get to the spatial resolution, which was set by the angular extent of the diffraction pattern, as high as possible, the diffraction signals were recorded at a distance of 4 cm, which was the nearest position from the specimen to the CCD chip. Second, eight diffraction patterns at high angle around the central diffraction signals were recorded by moving CCD perpendicularly to the beam. Parts of the diffraction signals intentionally overlap by 400 microns (the length of 20 pixels) between any two diffraction patterns. Then, the CCD was moved along the optical path to a distance of 22.65 cm such that the central diffraction speckle can be measured. At each position, two sets of diffraction signals were collected with the specimen in the beam and without the specimen but only with the cover slip in the beam.

III. Results

To mitigate the background noise effect, the blank signals were subtracted from each raw diffraction pattern at different positions. The high angle diffraction signals at 4 cm were tiled into a large diffraction pattern according to the overlap position. The size of the matrix of the pattern is 2001 × 2001, as shown in Fig. 2(b). Then the diffraction pattern at 22.65 cm was binned to make up the central speckle. The inset in Fig. 2(b) shows the central speckle of the diffraction pattern of which the center is obscured by the beam stop. The missing data was confined in a 7 × 7 matrix, which was smaller than the matrix of the central speckle, due to the central speckle is very significant in the reconstruction process. In order to enhance the signal-to noise-ratio, numerical integration of binning 3 × 3 pixels into 1 pixel was used to binned the diffraction pattern, which is helpful to reduce the dependence on the beam coherence and make the reconstruction fast. The binning criterion is that the linear oversampling ratio of the diffraction pattern after binned ≥2. Then the binned diffraction pattern was deconvoluted to remove the error due to intensity integration, as shown in Fig. 2(c) [7]. As to the dissatisfaction of paraxial condition, the diffraction pattern is obviously distorted at higher angles, as shown in Fig. 2(b). To remove the distortion, the planar diffraction pattern was interpolated onto the Ewald sphere to serve as a curvature corrected pattern, which is shown in Fig. 2(d).

Firstly, the image was reconstructed using Fig. 2(d). Because the specimen was a phase object, the difference map algorithm combined with shrink wrap method was used for iterative operation between the Fourier and the real space [9]–[10]. The original support was reconstructed from the autocorrelation of the sample [11]. In the real space, the value outside the support was set to be zero. And no constraints were set on the amplitude or phase of the sample. The reconstruction progress depended on the difference map iteration relationship. In the Fourier space, the square root of the diffraction intensity was employed in each iteration. The multiple scattering was not considered because the distance between any two spheres was long enough. Adding a broad Gaussian feature at the center of the support in the process of the reconstruction, the problem of missing data was overcome [10]. The support of the reconstruction was updated once every 100 iterations. A total of 400 iterations were performed, and a final image was obtained. Then the images of 100 reconstructions were averaged. The images of amplitude of the two independent 100 run images are shown in Fig. 3(a) and Fig. 3(b), respectively, which are in good agreement with each other and the microscope shown in Fig. 2(a). The line scan consistency of the two images in the same position is good along the white dashed line, as shown in Fig. 3(d), which confirms the good fidelity of the reconstruction. Fig. 3(c) was the averaged phase image of the specimen. The convergence of the reconstruction was identified by the error function, which is defined as:

$$Error = \frac{\sum ||F_c| - |F_m||}{\sum |F_m|} \tag{1}$$

where $|F_c|$ and $|F_m|$ are the calculated and the measured amplitude of the diffraction patterns. The reconstruction log error is shown in Fig. 4(a). After 100 iterations, the reconstruction terminated and the error function became relatively stabilized. Then the support was updated to a tighter one by shrink wrap method. The value of the error function decreased obviously from the 1st support to the 3rd support and changed a little from 3rd support to the 4th support. The size of each microsphere shown in Fig. 3(a) and Fig. 3(b) is the product of the number of

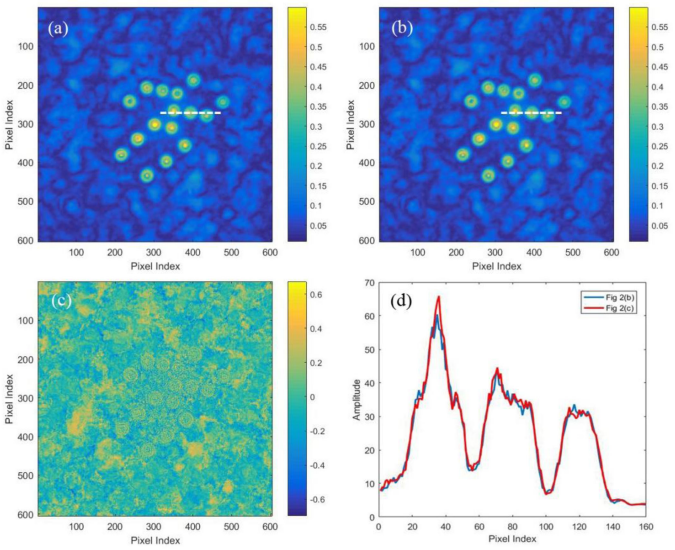

Fig. 3. Reconstruction results by difference map algorithm. Parts (a) and (b) are the two 100 times averaged independent reconstructed amplitudes. (c) 100 times averaged reconstruction phase. (d) Line scans along the white dashed lines in parts (a) and (b) show a good consistency of reconstruction.

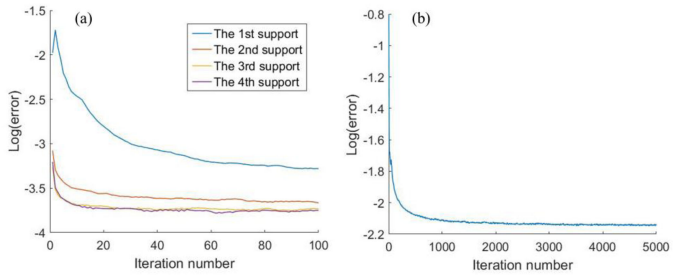

Fig. 4. (a) Convergence during the reconstruction by the diffraction pattern with curvature correction from the 1st support to the 4th support. (b) Convergence during the reconstruction by the diffraction pattern without curvature correction.

pixels and the image resolution so that the reconstructed images supplies the true size of all the spheres. The images of individual spheres were isolated by convoluting the amplitude image and set a cutoff value. The lateral resolution was calculated by the formula, $d_{x,y} = \lambda / \sin(2\theta)$, where λ is the wavelength and 2θ is the diffraction angle subtended by the distance from the center to the edge of the CCD. In our experiment, $\lambda = 543$ nm, and the distance from the center to the edge of the CCD was 2 cm. Thus the diffraction angle is 29 degrees, the resolution is 1.12 micron and the pixel size of the reconstructed image is 0.56 micron. Fig. 5(d) shows all the sizes of the microspheres, which were obtained without any priori information of the refractive indices. The largest microsphere's size is 24.08 microns, and the smallest microsphere's size is 20.16 microns.

The image was reconstructed secondly with Fig. 2(c) as a diffraction pattern, and the hybrid input-output (HIO) algorithm was used for iterative operation [12]–[13]. The diffraction pattern was reconstructed ten times independently and at every time 5000 iterations were run. The log error also defined by the function (1) of the reconstruction at one time is shown in

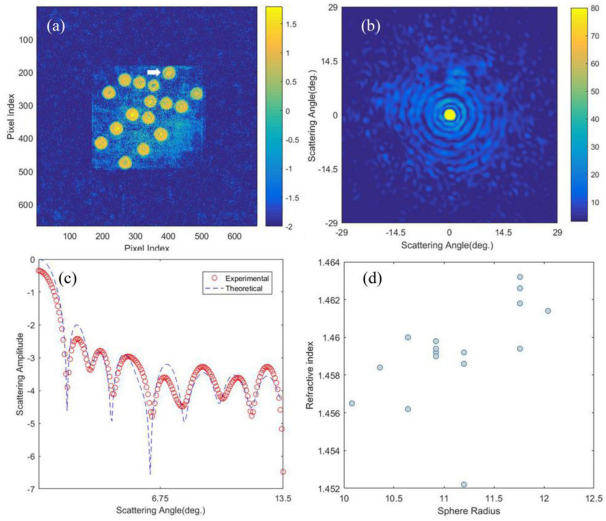

Fig. 5. (a) Ten times averaged amplitude of reconstruction by HIO algorithm. (b) Scattering amplitude of the sphere marked by the white arrow in part (a). (c) Comparison of the experimental and the Mie theory curve. (d) Radii and refractive indices of individual spheres.

Fig. 4(b). The image of the averaged amplitude is shown in Fig. 5(a). The amplitude and phase images of each microsphere were also isolated by convolution of the image and setting a cutoff value. The scattering amplitude of a single microsphere can be calculated by using 2D Fourier transform, as follows:

$$F(k_x, k_y) = \iint f(x, y) \exp(-2\pi i(k_x x + k_y y)) dx dy \quad (2)$$

where x and y are the spatial coordinates in real space, and k_x and k_y are the spatial-frequency coordinates in the Fourier space. The 2D scattering amplitude belonging to the microsphere which is marked by the white arrow in Fig. 5(a) is shown in Fig. 5(b) as an example, in which there are seven distinct concentric rings can be distinguished. The scattering amplitude curve was fitted by Mie theory to verify the feasibility of the technique, as shown in the Fig. 5(c). The sizes of the microspheres come from the first reconstruction. The theoretical curve calculated by the Mie theory was compared to the experimental curve and the refractive index was adjusted until the two curves displaying a compatible agreement. Therefore the refractive index of the microsphere, which is 1.4618, was obtained. The refractive index of all the microspheres is shown in Fig. 5(d). The maximum refractive index is 1.4632 and the minimum refractive index is 1.4522.

IV. Conclusion

In summary, we have experimentally proved that the angular scattering images, the sizes and the refractive indices of the individual microspheres can be retrieved simultaneously by the diffraction pattern of a specimen consisting of some spherical particles. The advantage of this technique is that it can obtain the sizes and the refractive indices of microspheres separately in order to reduce the ambiguity introduced by setting several parameters simultaneously. The image of the particles system

is reconstructed by the diffraction pattern after curvature correction and by the diffraction pattern without curvature correction, respectively. The image reconstructed by the diffraction pattern after curvature correction can provide the size of the microspheres. The amplitude and phase images reconstructed by the diffraction pattern without curvature correction can be used to obtain the angular scattering image of the individual microspheres by employing Fourier transform. And the refractive indices of the microspheres can be determined by perform comparison between the experimental curve and the calculation of Mie theory. In this work, we selected the system of microspheres as the specimen, which is because the feasibility of the technique is easy to be verified. However, we believe this technique can be straightforwardly extended to rapidly characterize a non spherical micro colloidal particles system. Moreover, we will realize this high angle scattering measurement by single shot in the future work using spatial-filter mirrors for detecting some active phenomena.

ACKNOWLEDGEMENT

The authors would like to thank Doctoral Foundation of Shandong Jianzhu University.

REFERENCES

[1] P. Ferrand *et al.*, "Direct imaging of photonic nanojets," *Opt. Exp.*, vol. 16, pp. 6930–6940, 2008.

[2] M. Giglio, M. Carpineti, and A. Vailati, "Space intensity correlations in the near field of the scattered light: A direct measurement of the density correlation function g(r)," *Phy. Rev. Lett.*, vol. 85, pp. 1416–1419, 2000.

[3] M. J. Berg, S. C. Hill, G. Videen, and K. P. Gurton, "Spatial filtering technique to image and measure two-dimensional near-forward scattering from single particles," *Opt. Exp.*, vol. 18, pp. 9486–9495, 2010.

[4] L. M. Shermann, and G. Alessandro, "High-resolution size measurement of single spherical particles with a fast Fourier transform of the angular scattering intensity," *App. Opt.*, vol. 35, pp. 4919–4926, 1996.

[5] H. Ding, Z. Wang, F. Nguyen, S. A. Boppart, and G. Popescu, "Fourier transform light scattering of inhomogeneous and dynamic structures," *Phys. Rev. Lett.*, vol. 101, pp. 238102-1–238102-4, 2008.

[6] M. J. Berg, and S. Holler, "Simultaneous holographic imaging and light-scattering pattern measurement of individual microparticles," *Opt. Lett.*, vol. 41, pp. 3363–3366, 2016.

[7] F. Ferri, "Use of a charge coupled device camera for low-angle elastic light scattering," *Rev. Sci. Instruments*, vol. 68, pp. 2265–2274, 1997.

[8] C. Song *et al.*, "Phase retrieval from exactly overspecimend diffraction intensity through deconvolution," *Phys. Rev. B*, vol. 75, pp. 012102-1–012102-4, 2007.

[9] V. Elser, "Phase retrieval by iterated projections," *J. Opt. Soc. Amer. A*, vol. 20, pp. 40–55, 2003.

[10] S. Marchesini *et al.*, "X-ray image reconstruction from a diffraction pattern alone," *Phys. Rev. B*, vol. 68, pp. 399–404, 2003.

[11] J. R. Fienup, and T. R. Crimmins, "Reconstruction of the support of an object from the support of its autocorrelation," *J. Opt. Soc. Amer.*, vol. 72, pp. 610–624, 1982.

[12] R. L. Sandberg *et al.*, "High numerical aperture tabletop soft X-ray diffraction microscopy with 70-nm resolution," in *Proc. Nat. Acad. Sci.*, USA, 2008, vol. 105, pp. 24–27.

[13] J. R. Fienup, "Phase retrieval algorithms: A comparison," *App. Opt.*, vol. 21, pp. 2758–2769, 1982.